

## FORMATION OF ORDERED ZnO STRUCTURES GROWN BY THE ALD METHOD ON HYBRID SiC/Si (100) SUBSTRATES

S.A. Kukushkin<sup>1-3\*</sup>, A.V. Osipov<sup>2</sup>, I.A. Kasatkin<sup>4</sup>, V.Y. Mikhailovskii<sup>4</sup>, A.I. Romanychev<sup>4</sup>

<sup>1</sup>Institute of Problems of Mechanical Engineering, Russian Academy of Sciences, St. Petersburg, Russia

<sup>2</sup>ITMO University, St. Petersburg, Russia

<sup>3</sup>Peter the Great Saint Petersburg State Polytechnic University, St. Petersburg, Russia

<sup>4</sup>St. Petersburg State University, St. Petersburg, Russia

\*e-mail: sergey.a.kukushkin@gmail.com

**Abstract.** Crystalline structure and composition of the ZnO films grown by atomic layer deposition (ALD) on the n- and p-type Si (100) substrates with a SiC buffer layer were studied. The SiC buffer layers have been synthesized by a novel method of atomic substitution (partial chemical replacement) of Si atoms by carbon atoms in the subsurface layer of the Si substrate. A four-component epitaxial texture of ZnO in a direction close to [101] on the n- and p-type (100) Si vicinal substrates with a SiC buffer layer has been revealed and investigated with electron diffraction. Formation mechanism of the epitaxial textures of ZnO was found to depend on the conductivity type (n- or p-type) of the Si (100) substrates. A theoretical model explaining the effect of the texture formation and its dependence on the type of Si substrate conductivity has been proposed. The effect is associated with the transformation of the vicinal Si (100) surfaces into the SiC surfaces during its synthesis by the atomic substitution method. Significant differences have been found between the structures and between the growth mechanisms of the ZnO layers on the SiC/Si (111) and (100) substrates.

**Keywords:** zinc oxide films, ALD method, silicon carbide; epitaxy; thin film growth

### 1. Introduction

This work continues the previous studies [1] of the growth of the zinc oxide (ZnO) films by atomic layer deposition (ALD) on silicon (Si) substrates with silicon carbide (SiC) buffer layers grown by the method of topochemical substitution of atoms [2-4]. Zinc oxide, as is well known, crystallizes in a hexagonal lattice system with lattice parameters  $a = 0.325$  nm and  $c = 0.521$  nm. The Silicon carbide films on the silicon surfaces, which are the substrate for the ZnO layer, were synthesized by the atomic substitution method. Depending on the crystallographic orientation, the Si surfaces can consist of both layers of the cubic SiC phase and layers of the hexagonal phase [5]. On the Si (111) surface, essentially a cubic polytype of 3C-SiC is formed [5], on the Si (110) surface, mainly hexagonal polytypes grow, with the 6H-SiC polytype being basically formed and, to a lesser degree, the 4H-SiC polytype [5]. A film consisting of a mixture of various SiC polytypes grows on the (100) Si surface. In [6], it was found that the structure of the surface SiC layers synthesized on the vicinal surfaces of Si (100) substrates deviating from the basic orientation by  $2^\circ - 7^\circ$  substantially depends on the doping type of the initial silicon substrate. It turned out [6] that in the process of replacing silicon atoms with carbon atoms, singular (100) Si faces transform into a SiC face consisting

of an ensemble of facets resembling sawtooth structures, whose lateral surfaces are covered with (111) planes. These studies showed that on the vicinal p-type Si surface, deviated by  $4^\circ$  and more from the singular face (100) during the synthesis of SiC, an ordered phase of SiC is formed, with surface morphology in the form of facets (flakes) consisting of cubic and hexagonal layers. In this case, the planes of the hexagonal facets may have the orientation:  $[\bar{1}10\bar{2}]$ ;  $[\bar{1}100]$ ;  $[\bar{1}10\bar{1}]$ . Cubic facets consist of (111) faces and are positioned at an angle of  $54^\circ44'$  to the (100) face. If initially the vicinal surface of the Si (100) substrate was prepared from Si cut at an angle of  $4^\circ$  to the surface (100), for example, towards [011], then after thermal annealing [3,6], such a surface will be covered with an ensemble of steps (011). After topochemical transformation of this surface into the SiC surface, it would be covered by an ensemble of facets with (111) planes (111) located at an angle of  $54^\circ44'$  to the (100) face. Moreover, all facets will be ordered along the [011] direction at an angle of  $\approx 35^\circ$  to the (001). Thus, during the synthesis of SiC, a modified SiC surface is formed, structured along the [011] direction. As shown by earlier studies [7], Si substrates with a SiC layer structured in a similar way are good templates for the growth of semi-polar hexagonal AlN and GaN crystals. Such a quasi-stepped surface of a silicon carbide layer stimulates the formation of nuclei of hexagonal semi-polar AlN, and the semi-polar layer of AlN, that in turn stimulates the formation of a semi-polar GaN layer, for example, the  $(1\bar{1}01)$  GaN plane is located at an angle of  $35\text{--}47^\circ$  with the "C" GaN axis and the (001) SiC plane.

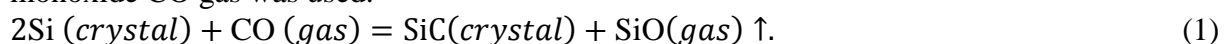
On the vicinal n-type Si surface deviated by an angle of  $4^\circ$  or more from the singular (100) face, the process during the synthesis of SiC proceeds differently. On this surface, only the 3C-SiC cubic phase is formed, and the density of the (111) facets is not large, and they are very small. As a result, polycrystalline AlN and GaN films grow on vicinal n-type Si surfaces, as a rule, when grown by the method of chloride-hydride epitaxy (HVPE), because the substrate has very few orienting centers, and the differences between the SiC lattice parameters in the plane (100) and the lattice parameters of GaN along its semipolar planes, for example  $(1\bar{1}01)$ , are rather large. It was shown in [8] that in order to grow semipolar AlN and GaN layers on the faceted the SiC/Si(100) surface, it is necessary to create an AlN nucleus, whose critical size would not exceed the size of the SiC facet. This requires a high growth rate of the AlN layer of the order of  $1\text{ }\mu\text{m}/\text{hour}$ . Otherwise, the polar AlN and GaN layers will grow, which on the SiC/Si (100) surface will have a polycrystalline structure.

In this connection, it is of great interest to find out the differences in the morphology and structure of ZnO layers grown on n and p type Si (100) substrates with a SiC buffer layer. Such a study is very important for finding out the mechanism of growth of the ZnO layer on SiC/Si (100). It should be noted that for comparison, we present some data on the formation of ZnO on SiC grown on Si (111). In this work, we do not consider growth on a pure silicon substrate in since as was shown in [1], ZnO films grown by the ALD method on Si have a polycrystalline structure.

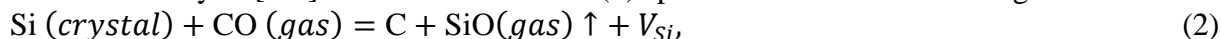
Thus, the aim of the present work is to study the morphology and crystal structure of ZnO layers grown by the ALD method, depending on the orientation of the initial Si substrate and the type of its conductivity.

## 2. Experimental technique

The epitaxial SiC layer was grown on vicinal surfaces, with a deviation of  $4^\circ$  from the (100) plane, of the n- and p-type Si (100) substrates. Silicon substrates with a resistivity of  $10\text{ }\Omega\cdot\text{cm}$  were used for SiC growth. The growth of SiC was carried out using the new method of chemical substitution of atoms developed in [2–4]. To synthesize a SiC layer by this method, following to [2–4], a topochemical reaction between the single-crystal Si substrate and carbon monoxide CO gas was used.



The analysis [2-4] showed that reaction (1) splits into two successive stages.



Silicon vacancies  $V_{\text{Si}}$  play a key role at both stages of transformation [2–6]. In the first stage of reaction (2), they ensure not only the diffusion of the CO reagent to the reaction zone, but also the reaction product of SiO from the reaction zone. In addition, the C atom and the vacancy  $V_{\text{Si}}$ , which are formed in pairs in stage (2), have a strong interaction with each other, caused by the overlapping of elastic fields in a medium with cubic symmetry, to which silicon crystal belongs [2-5]. In particular, if these pairs align along the [111] direction, which corresponds to an energy minimum, they form a stable configuration, which we call dilatation dipoles by analogy with electric dipoles. In fact, silicon saturated with such dilatation dipoles (4 dipoles per Si cell) is an intermediate complex or an intermediate phase for almost barrier-free conversion into silicon carbide [9]. Since the SiC cell volume is two times smaller than the Si cell volume, the presence of vacancies here also plays a key role, providing a barrier-free displacement of large regions of the crystal.

Topochemical reaction (1) proceeded in a vacuum furnace at a temperature  $T = 1280^\circ\text{C}$  and a pressure of CO  $p_{\text{CO}} = 0.4$  Torr for 25 min. An epitaxial SiC film with a thickness of about 50 nm was formed from a mixture of predominantly hexagonal 4H and 6H polytypes [5]. Under the SiC film in the Si bulk, voids and cavities were formed, caused by the evolution of an ensemble of dilatation dipoles and merely silicon vacancies. They do not affect the SiC quality.

Then, ZnO films were deposited on the obtained Si templates with a buffer layer of SiC by the method of molecular layering. Zinc oxide, as in [1], was obtained by molecular layering [1,10,11] using diethyl zinc ( $\text{Zn}(\text{C}_2\text{H}_5)_2$ ) reagents and deionized water ( $\text{H}_2\text{O}$ ). These substances, having a sufficiently high vapor pressure, were alternately supplied in a stream of nitrogen, which served as the carrier gas. When a substrate was exposed to water vapor, an adsorbed phase of the corresponding OH groups forms on it. During subsequent exposure to diethyl zinc, ZnO structural units are formed on the substrate due to the interaction with OH groups. The sum of these two stages is described by the reaction



At a given flow of reagents, the temperature is chosen so that the reagent excess, together with the reaction product  $\text{C}_2\text{H}_6$ , have time to leave the reactor. The substrate temperature was  $250^\circ\text{C}$ . Reactions occur on the substrate surface at high speed, so the film growth is determined mainly by the speed of delivery of the reagent molecules from the gas phase to the substrate surface. The substrate processing time in reagent vapors was  $10^{-2} - 5 \cdot 10^{-2}$  s, purge time was 4-5 s. Thus, the deposition time of one monolayer (one reaction cycle) was about 8–10 s. The thickness of the ZnO films was  $\sim 200$  nm.

The grown ZnO films were studied by scanning electron microscopy, elemental microanalysis, X-ray diffraction and reflection high-energy electron diffraction (RHEED). Elemental analysis and scanning microscopy of the films were carried out on a Zeiss Merlin microscope with a thermopole-left cathode, equipped with an analytical attachment for energy dispersive elemental microanalysis of Oxford Instruments INCA X-Act. The accelerating voltage of the electron beam was 10 kV, and the beam current was 220 pA. An Everhart-Thornley detector and a semiconductor back-scattered electron detector were used to record the images. X-ray diffraction studies were performed with a D8 Discover high resolution diffractometer (Bruker AXS) using a parallel beam of filtered  $\text{CuK}_\alpha$  radiation with a point focus and a spot diameter of 0.5 mm. To obtain electron diffraction data, we used an EMR-100 electron diffractometer with an electron energy of 50 keV.

### 3. Research results

**Scanning electron microscopy and elemental analysis.** Figure 1 shows the image of the end sections of the ZnO/SiC /Si (100) samples grown on n-type and p-type Si obtained using a scanning electron microscope.

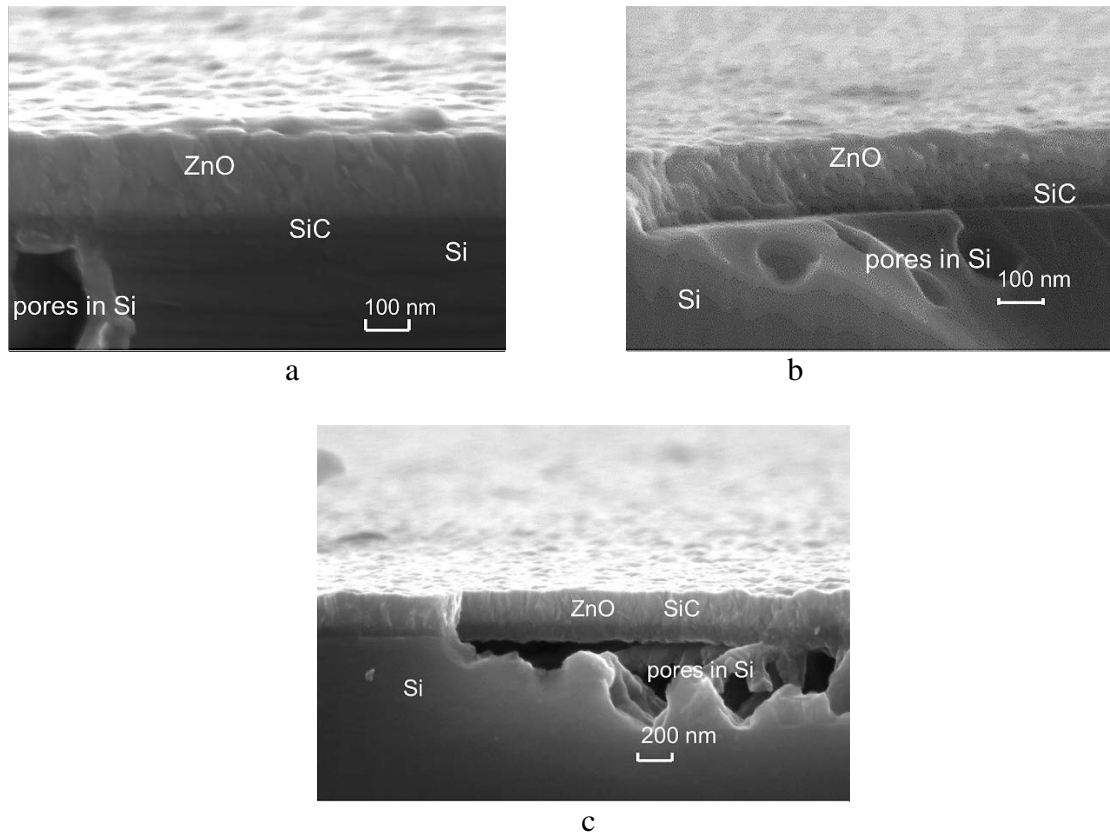


**Fig. 1.** SEM images of the end cut of ZnO/SiC/Si(100) samples and ZnO/SiC/Si (111) samples; (a) on n-type Si (100); (b) on p-type Si (100); (c) on Si (111) of n, p-type conductivity, obtained with a scanning raster electron microscope. Under the SiC layer, pores and voids in the volume of Si are seen

On a SiC/Si (100) n-type substrate, a ZnO layer with a thickness of about 170 nm has grown. The thickness of the ZnO layer on a SiC / Si(100) p-type substrate was about 230 nm. The thicknesses of the ZnO layers on SiC /Si(111) n-type and p-type substrates were of the order of 250 nm. The thickness of the SiC layer on n-type Si (100) was ~ 50 nm, the thickness of the SiC layer on p-type Si (100) was ~ 60 nm, the thickness of the SiC layers on n- and p-type Si (111) substrates were ~ 110 nm. Under the SiC layer there are pores in the bulk of the silicon substrate, which were formed as a result of the topochemical reaction (2) and (3). Figure 2 presents the results of X-ray fluorescent microanalysis of the ZnO film composition. X-ray fluorescence analysis was performed at various points of the ZnO film, namely: on its surface, in the middle part of the ZnO layer, at the interface of the ZnO film with the SiC film, in the middle part of the SiC layer, at the interface of the SiC layer with the Si substrate, and approximately at a distance of about 1  $\mu\text{m}$  from the SiC–Si interface into the depth of the silicon substrate. The analysis showed that ZnO films grown on SiC/Si (100) substrates of both n-type and p-type are stoichiometric. The atomic content in the ZnO layer grown on an n-type substrate is the following: Zn = 26.5%, oxygen O = 17.2%, silicon Si = 19.3%, carbon C = 37%. The content of the same atoms in the ZnO layer grown on an p-type substrate is Zn = 25.8%, oxygen O = 17.7%, silicon Si = 19.3%, carbon C = 37%. ZnO films grown on

SiC/Si(111) n-type and p-type substrates contained above given atoms in the following composition: Zn = 25.6%, O = 17.8%, Si = 18.7%, C = 37.9%. Note that the concentration of silicon and carbon in this case should not be taken into account, since during microanalysis, the electron beam penetrates to a depth exceeding the thickness of the ZnO films. The excess carbon concentration in comparison with silicon only means that there is a SiC layer between the ZnO layer and Si. The analysis carried out by us showed that the Zn/O ratio is higher for the ZnO sample on an n-type substrate, i.e. oxygen concentration is greater in samples grown on a p-type substrate. This means that the concentration of oxygen vacancies is somewhat higher in a ZnO film grown on an n-type substrate. As is known, oxygen vacancies are electron donors. However, this difference is comparable with the magnitude of the error of the method.

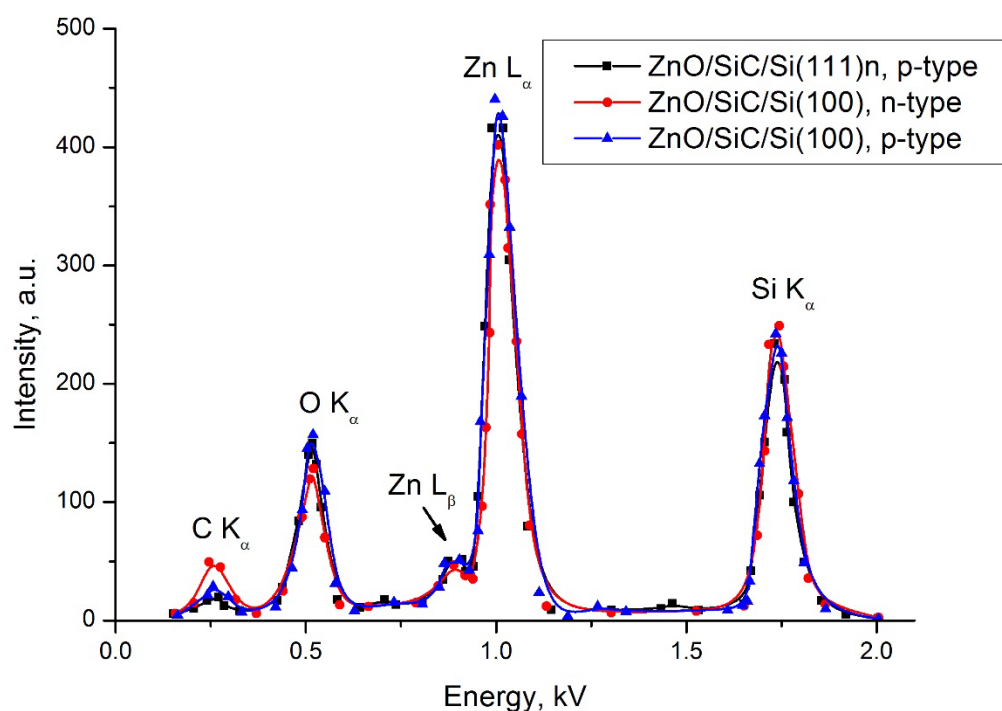


**Fig. 2.** X-ray fluorescence analysis spectra for  $K_{\alpha}$  and  $L_{\beta}$  lines showing the content of Zn, O, C, and Si in the center of the ZnO layer grown on SiC/Si (100) and SiC/Si (111) samples with n- and p-type silicon

**X-ray diffraction studies.** X-ray diffraction studies showed that on the SiC sublayers grown on n-type and p-type Si (100) and Si (111) substrates a uniaxial three-component ZnO texture along the [101], [001] and [hk0] directions was formed (in the latter case the [hk0] directions were oriented along the surface normal, and the [001] directions of crystallites were parallel to the surface and had random azimuthal orientations). A typical image of X-ray reflections of such a "background" uniaxial texture is shown in Fig.3.

An epitaxial texture along the direction close to [101] was superimposed on the background uniaxial zinc oxide texture. The  $2\theta$ - $\chi$  diagrams of the ZnO layers grown on the SiC/Si (100) substrates of the n- and p-type conductivity are shown in Fig.4.

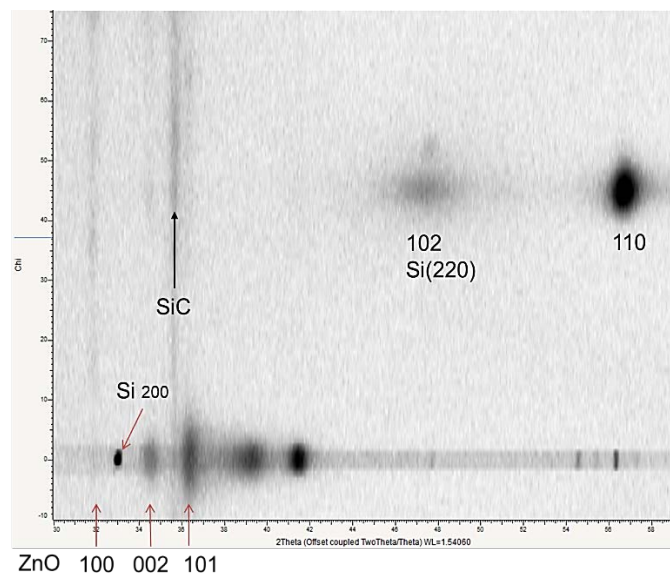


**Fig. 3.** A typical series of symmetrical  $\theta$ - $2\theta$  scans for different tilt angles  $\chi$  of a ZnO layer grown on a SiC/Si(100) substrate with either n-type or p-type silicon. sample. The background texture maxima of ZnO are visible at  $\chi = 0$  ( $\parallel [101] + \parallel [001]$ ). A  $\chi$ -profile of such a diagram at a given Bragg angle ( $2\theta$ ) represents a meridional profile of the corresponding pole figure

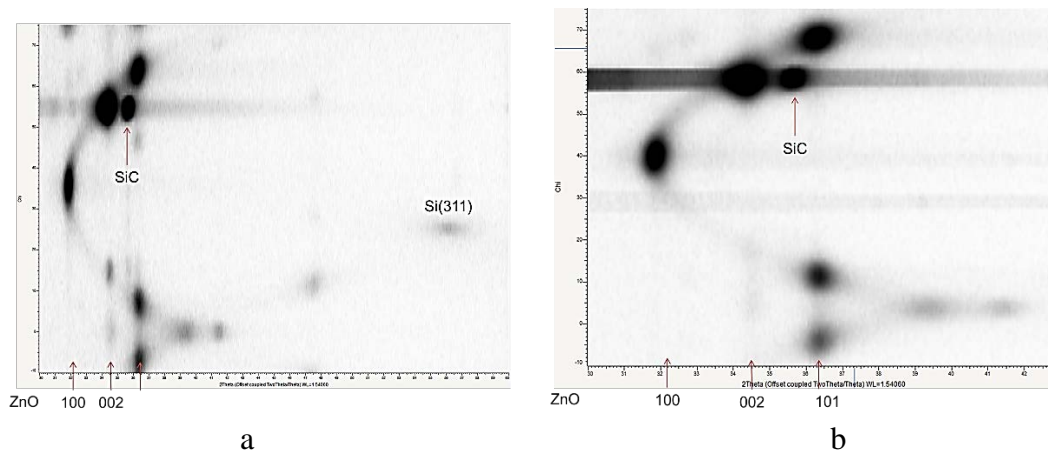


**Fig. 4.** A series of symmetrical  $\theta$ - $2\theta$  scans for various tilt angles  $\chi$  of ZnO samples grown on the SiC/Si (100) substrates; (a) Si (100) n-type; (b) Si (100) p-type. The epitaxial texture maxima are visible

The combined pole figure of the ZnO/SiC/Si (100) sample grown on n-type Si (100) is shown in Fig. 5.

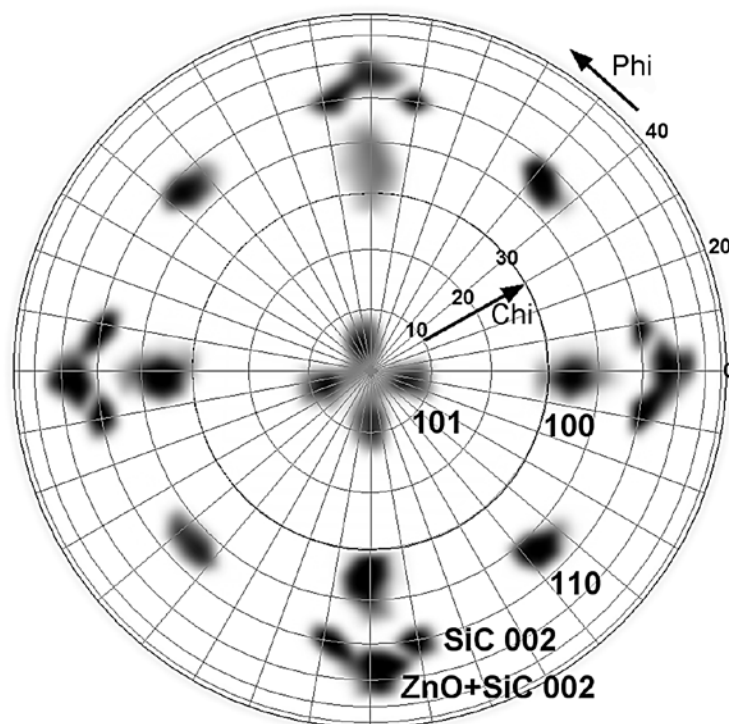
Figure 5 clearly shows the relatively sharp texture maxima of SiC and ZnO, which are characteristic of epitaxial textures. For the ZnO/SiC /Si (100) sample grown on the p-type Si (100) the combined PF is similar.

Figure 6 shows the  $2\theta$ - $\chi$  diagrams for the ZnO layer (texture  $\parallel [101] + \parallel [001]$ ) grown on the SiC/Si(111) substrates with n- and p-type silicon.

For all samples, the profiles of the texture maxima for the main directions ( $\chi$  scans) were obtained, and the peaks were fitted with the Gaussian functions. Full widths of these curves at half maximum (FWHM) measured with a standard error of about 1% characterize the texture sharpness. The ZnO [101] texture maximum had FWHM  $\approx 5.4^\circ$  on the SiC/Si (100) substrate with the n-type conductivity. On a SiC/Si (100) substrate with the



p-type conductivity the same texture has a sharpness of  $4.9^\circ$ . On the other hand, the sharpness of the ZnO texture along the [001] direction on the SiC/Si (100) substrate with the n-type conductivity was  $5.10^\circ$ , which is similar to that on the p-type silicon ( $5.3^\circ$ ). On the n-type SiC/Si (111) substrates the ZnO texture had a sharpness of  $6.30^\circ$  and  $4.5^\circ$  along the [101] and [001] directions, correspondingly. On the p-type SiC/Si (111) substrate the texture sharpness was as large as  $7.2^\circ$  in the [101] direction and only  $4.5^\circ$  in the [001] direction.



**Fig. 5.** The combined pole figure for the ZnO/SiC/Si (100) sample grown on the n-type Si (100). The angle  $\chi$  varied from 0 to  $+70^\circ$  in the process of measurement

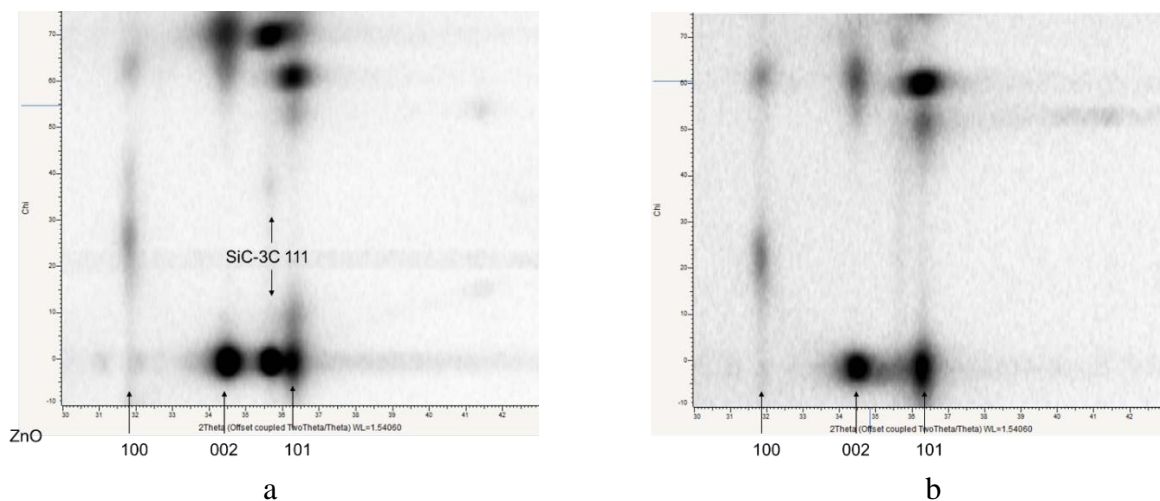


**Fig. 6.** A series of symmetrical  $\theta$ - $2\theta$  scans for various tilt angles  $\chi$  of ZnO samples with texture  $\parallel [101] + \parallel [001]$  grown on SiC/Si(111) substrates. (a) - n-type conductivity; (b) - p-type conductivity

**Electron diffraction studies.** Figure 7 shows the RHEED pattern obtained from the surface of ZnO samples formed on SiC grown on n- and p-type Si (100), obtained on an EMR-100 electron diffraction image at 50 keV electron energy. Diffraction patterns are

shown along two directions, namely, along the projection of the [001] axis and in the projection of the [011] axis. As is known, while registering a RHEED pattern, electrons with an energy of 50 keV penetrate into the film layer to a depth not exceeding 30–50 nm, while X-ray beams penetrate much deeper. Therefore, RHEED is appropriate to investigate the structure of the surface layers, which may differ from the structure averaged over the entire thickness of the layer, which was studied by X-ray diffraction. Above, we showed that the ZnO layer is textured, with some order along the [101] and [001] directions. As a rule, with an increase in the film thickness, if the substrate has ordering centers, the degree of film crystallinity may increase [12]. This is what we observe in Fig. 7. For the ZnO layer grown on a n-type Si (100) substrate as well as for the ZnO layer grown on a p-type Si (100) substrate, there is a gradual transformation from texture to epitaxial orientation. So, in Fig. 7a and Fig. 7c it is clearly seen that the ZnO epitaxial layer starts to form along the [001] axis at the surface of SiC samples grown on a n-type Si substrate as well as on a p-type Si substrate. The reflexes are still quite diffused, though there are reflexes indicating the presence of the twin phase. However, in general, an epitaxial structure has already been formed in this zone. Moreover, within the experimental error, this structure is more ordered for a sample grown on an n-type substrate. This result coincides with the result of our research of the FWHM of the texture profiles. Studies of electron diffraction patterns in the projection onto the axis of the [101] zone (Fig. 7b and Fig. 7d) show that the ZnO sample grown on an n-type substrate in this direction is only a slightly ordered texture. On the other hand, the structure of the ZnO layer grown on the p-type substrate along the [101] direction is more ordered than the structure of the ZnO layer on the n-type substrate. Despite the diffusion of reflexes, this surface is closer to the epitaxial one than to the textured surface. This result also coincides with the result of our research of the FWHM of the texture profiles.

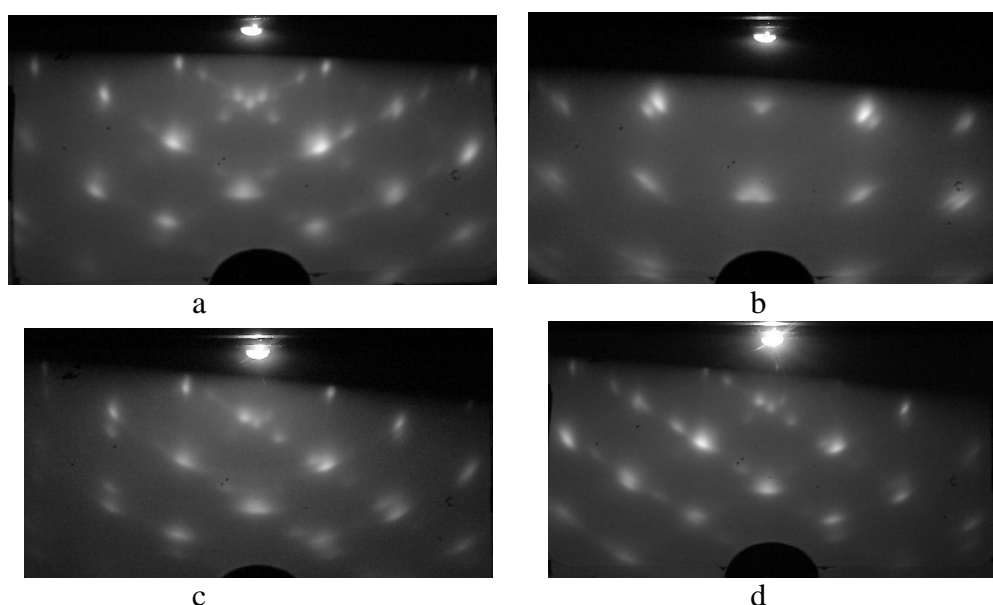


**Fig. 7.** RHEED patterns from ZnO samples formed on SiC grown on n- and p-type Si (100) obtained in two directions; in the projections of the [001] and [101] and axes (a) – n-type Si (100) in the [001] direction; (b) – n-type Si (100) in the [011] direction; (c) – p-type Si (100) in the [001] direction; (d) – p-type Si (100) in the [101] direction

Figure 8 shows RHEED patterns for reflection from the surface of ZnO samples formed on SiC of SiC on n- and p-type Si (111).



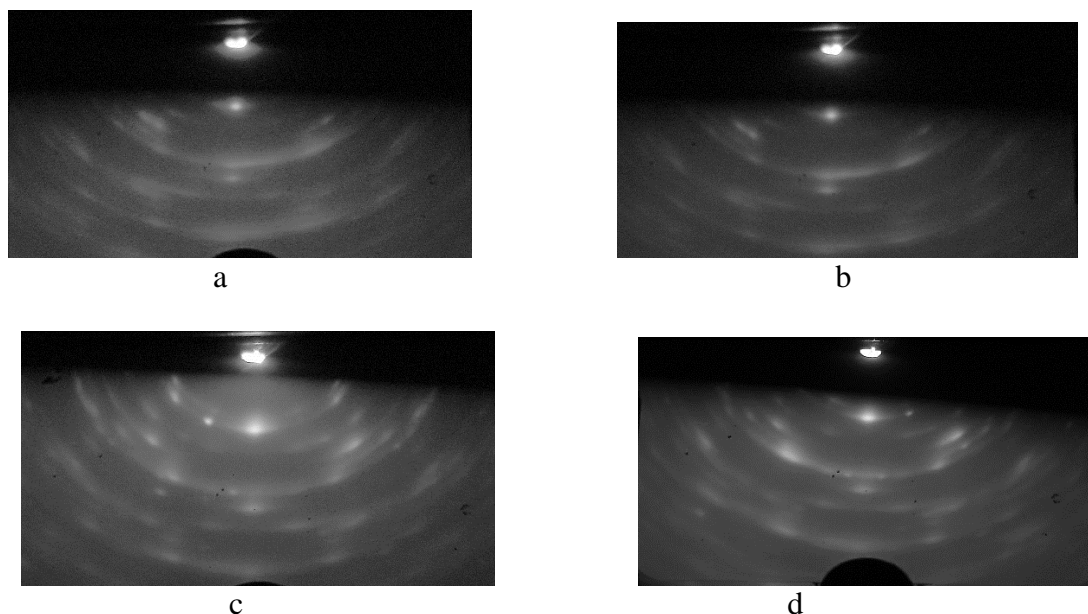


**Fig. 8.** RHEED patterns from ZnO samples grown on SiC on n- and p-type Si (111) registered along two directions; in the projection of the [001] axis and in the projection of the [101] axis.

(a) – n-type Si (111) in the [001] direction; (b) – n-type Si (111) in the [011] direction; (c) p-type Si (111) in the [001] direction; (d) – p-type Si (111) with p-type conductivity in the [101] direction

From the data shown in Fig. 8, it follows that the ZnO layers lying near the surface of the ZnO/SiC/Si (111) films are textured both in the direction of the [001] zone axis and in the direction of the [101] axis regardless of the type of the substrate conductivity. The appearance of a larger number of diffused point reflections in Fig. 8c and Fig. 8d as compared with the reflexes in Fig. 8a and Fig. 8b can be attributed, in our opinion, to the experimental error. It is important to note the following. The ZnO layers grown on SiC/Si (111) are much less ordered than the ZnO layers grown on SiC/Si (100) substrates. Averaging the FWHM profiles along the [001] and [101] directions also confirms this conclusion.

#### 4. Conclusion

Thus, in the present work, it was proved that the surface of SiC films grown by replacing Si (100) atoms is covered by an ensemble of ordering centers, i.e. crystal facets. In this case, as was previously theoretically shown [6], the facets on the vicinal surface of p-type Si are ordered and consist of layers of both cubic and hexagonal phases. This structure of SiC layers affects a strong ordering effect on the growth of epitaxial layers of crystals crystallizing in hexagonal symmetry. Thus, in the present study, we unambiguously showed that SiC/Si (100) hybrid substrates synthesized by the method of topochemical substitution of atoms for p-type Si, have ordering effects not only on the AlN and GaN layers growing by the HVPE method at high synthesis temperatures, but also on ZnO layers synthesized by the ALD method at low synthesis temperatures (about 250°C). Thus, the facet formation on the surface of SiC films grown by the method of topochemical substitution of atoms on Si (100) leads to the removal of the degeneracy of the surface symmetry and the formation of growth centers of ZnO films along certain directions.

**Acknowledgements.** This work was supported by the Russian Science Foundation (Grant No. 14-12-01102). The synthesis of films by the ALD method, electron microscopic and X-ray diffraction studies were performed using the equipment of the resource centers of the Scientific Park of St. Petersburg State University "Nanotechnology", "X-ray diffraction

*methods of research", and "Innovative technologies of composite nanomaterials". The growth of SiC layers and the study of their properties were carried out using a unique scientific setup "Physics, Chemistry, and Mechanics of Crystals and Thin Films" (IPMash RAS, St.Petersburg).*

## References

- [1] Kukushkin SA, Osipov AV, Romanychev AI. Epitaxial Growth of Zinc Oxide by the Method of Atomic Layer Deposition on SiC/Si Substrates. *Phys. Sol. State*. 2016;58(7): 1448-1452.
- [2] Kukushkin SA, Osipov AV. A new method for the synthesis of epitaxial layers of silicon carbide on silicon owing to formation of dilatation dipoles. *J. Appl. Phys.* 2013;113: 024909.
- [3] Kukushkin SA, Osipov AV. Quantum mechanical theory of epitaxial transformation of silicon to silicon carbide. *J. Phys. D: Appl. Phys.* 2017;50: 464006.
- [4] Kukushkin SA, Osipov AV, Feoktistov NA. Synthesis of Epitaxial Silicon Carbide Films through the Substitution of Atoms in the Silicon Crystal Lattice: A Review. *Phys. Sol. State*. 2014;56(8): 1507-1535.
- [5] Kukushkin SA, Osipov AV. Determining Polytype Composition of Silicon Carbide Films by UV Ellipsometry. *Techn. Phys. Lett.* 2016;42(2): 175-178.
- [6] Kukushkin SA, Osipov AV, Soshnikov IP. Growth of epitaxial SiC layer on Si (100) surface of n- and p- type of conductivity by the atoms substitution method. *Rev. Adv. Mater. Sci.* 2017;52: 29-42.
- [7] Bessolov VN, Konenkova EV, Kukushkin SA, Osipov AV, Rodin SN. Semipolar gallium nitride on silicon: Technology and properties. *Rev. Adv. Mater. Sci.* 2014;38: 75-93.
- [8] Bessolov VN, Zubkova AV, Konenkova EV, Konenkov SD, Kukushkin SA, Orlova TA, Rodin SN, Rubets VP, Kibalov DS, Smirnov VK. Semipolar GaN(10–11) Epitaxial Layer Prepared on Nano-Patterned SiC/Si(100) Template. *Phys. Status Solidi B*. 2018;256: 1800268.
- [9] Kukushkin SA, Osipov AV. First-Order Phase Transition through an Intermediate State. *Phys. Sol. State*. 2014;56(4): 792-800.
- [10] Tynell T, Karppinen M. Atomic layer deposition of ZnO: A Review. *Semicond. Sci. Technol.* 2014;29(4): 043001.
- [11] Akopyan IK, Davydov VY, Labzovskaya ME, Labzovskaya ME, Lisachenko AA, Mogunov YA, Nazarov DV, Novikov BV, Romanychev AI, Serov AY, Smirnov AN, Titov VV, Filosofov NG. Photoluminescence Spectra of thin ZnO films grown by ALD technology. *Phys. Sol. State*. 2015;57(9):1865-1869.
- [12] Kukushkin SA, Osipov AV. Nucleation kinetics of nano-films. In: Nalwa HS. (ed.) *Encyclopedia of Nanoscience and Nanotechnology*. Vol. 8. American Scientific Publication; 2004. p.113-136.